ARMY RESEARCH LABORATORY

Modeling of a Magnetic Flux Concentrator

by Gregory A. Fischer and Alan S. Edelstein

ARL-TR-3166   **March 2004**

NOTICES

Disclaimers

Army Research Laboratory
Adelphi, MD 20783-1145

ARL-TR-3166   **March 2004**

Modeling of a Magnetic Flux Concentrator

Gregory A. Fischer and Alan S. Edelstein
Sensors and Electron Devices Directorate, ARL

REPORT DOCUMENTATION PAGE			Form Approved OMB No. 0704-0188

1. REPORT DATE (DD-MM-YYYY)	2. REPORT TYPE	3. DATES COVERED (From - To)
March 2004	Final	10/02–09/03

4. TITLE AND SUBTITLE	5a. CONTRACT NUMBER
Modeling of a Magnetic Flux Concentrator	5b. GRANT NUMBER
	5c. PROGRAM ELEMENT NUMBER

6. AUTHOR(S)	5d. PROJECT NUMBER
Gregory A. Fischer and Alan S. Edelstein	3NRERR
	5e. TASK NUMBER
	5f. WORK UNIT NUMBER

7. PERFORMING ORGANIZATION NAME(S) AND ADDRESS(ES)	8. PERFORMING ORGANIZATION REPORT NUMBER
U.S. Army Research Laboratory Sensors & Electron Devices Directorate (ATTN: AMSRL-SE-SS) gfischer@arl.army.mil Adelphi, MD 20783-1145	ARL-TR-3166

9. SPONSORING/MONITORING AGENCY NAME(S) AND ADDRESS(ES)	10. SPONSOR/MONITOR'S ACRONYM(S)
DARPA 3701 N. Fairfax Dr. Arlington VA. 22203-1714	11. SPONSOR/MONITOR'S REPORT NUMBER(S)

12. DISTRIBUTION/AVAILABILITY STATEMENT

Approved for public release; distribution unlimited.

13. SUPPLEMENTARY NOTES

14. ABSTRACT

Using the Maxwell 3-D finite element analysis software package from Ansoft, ARL performed magnetic modeling of the Visidyne flux concentrator. Visidyne Corp. has investigated using the Faraday effect to develop a high sensitivity vector field magnetometer. Laser light is sent down a hole in permalloy rods and passes through a single crystal of Yttrium-Iron-Garnet (YIG). Small changes in the surrounding magnetic field result in minute changes in the polarization of the light as it passes through the YIG. The permalloy rods act as flux concentrators, but the YIG crystal is not only part of the magnetic field sensor but also an integral part of the flux concentrator itself. We modeled the Visidyne flux concentrator in order to determine the enhancement factor given the dimensions, materials, and relative permeability of their materials. This factor was found to be 361 to 365. Variations in relative permeability of the permalloy as well as changes in the dimensions of the permalloy parts were also modeled. It was determined that changes in dimensions had an impact on the enhancement factor, allowing us to obtain a factor of 509. It was also shown that, if possible, an increase in the relative permeability of the YIG crystal could produce enhancement values in excess of those produced by changes in dimensions.

15. SUBJECT TERMS	Magnetic modeling, flux concentrator				

16. SECURITY CLASSIFICATION OF:			17. LIMITATION OF ABSTRACT	18. NUMBER OF PAGES	19a. NAME OF RESPONSIBLE PERSON
a. REPORT	b. ABSTRACT	c. THIS PAGE	SAR	23	Gregory A. Fischer
UNCLASSIFIED	UNCLASSIFIED	UNCLASSIFIED			19b. TELEPHONE NUMBER (Include area code) (301) 394-2089

Standard Form 298 (Rev. 8/98)

Contents

Figures

Tables

Executive Summary

We performed magnetic modeling of a new and novel magnetic sensor from Visidyne Corp. The sensor is a high sensitivity vector field magnetometer. Such sensors have considerable potential for use as unattended ground sensors (UGS), alone or networked with other types of sensors, and to detect underground facilities. At frequencies over 10 Hz, the Visidyne sensor sensitivity of 5pT/√Hz makes the sensor promising for UGS type applications. Below this frequency the sensor is limited by geomagnetic noise. Still higher sensitivity is desired for the detection of underground facilities. Optimizing the sensor will allow it to be better suited to the U.S. Army's needs. One way to improve the sensor is to optimize the flux concentrator that is incorporated in the sensor system. Increasing the enhancement of the magnetic field at the sensor due to the flux concentrator would result increase the sensor's sensitivity.

Magnetic modeling of the sensor and the flux concentrator allows us to alter dimensions and properties of materials and determine the corresponding change in the effectiveness of the flux concentrator without large outlays of time and money. We started with the dimensions and material properties that Visidyne quoted to us. Variations in material properties were tried while maintaining the dimensions of the flux concentrator. Calculated enhancements were compared to the calculated enhancement of Visidyne's original flux concentrator. Calculations were also performed in which the flux concentrator dimensions were varied while keeping material properties constant. This systematic approach allowed us to determine the extent that the performance of the flux concentrator could be improved to make the overall sensor performance more suitable for satisfying the U.S. Army's needs. With Visidyne's design, an enhancement factor of 361 to 365 could be expected. Changes in flux concentrator dimensions lead to an enhancement factor of 509. It was also shown that, if it could be obtained, the use of a YIG crystal with a permeability of 160 would lead to an enhancement of 1,095.

INTENTIONALLY LEFT BLANK

1. Introduction

A flux concentrator is a magnetically conductive material that provides an "easier" path for the magnetic flux to travel through. Such materials are soft ferromagnets with a high permeability [1]. As flux concentrators can direct, control, and focus the magnetic fields into a specific area, they are often used in magnetic sensor design. Thus, a small perturbation in the magnetic field is magnified by the flux concentrator, enabling a sensor to detect the perturbation [2,3]. The design of a flux concentrator is determined by size limitations of the sensor package as well as the amount of field magnification desired at the sensor. The type of magnetic sensor used can also affect the design of the flux concentrator. In this report we will be discussing the flux concentrator used by Visidyne Inc. as a part of their magneto-optical magnetic field sensor. Particular attention will be paid to what role material properties and dimensions play in the overall enhancement of the magnetic field at the sensor.

2. The Visidyne Flux Concentrator Design

Visidyne Corp. has investigated using the Faraday effect to develop a high sensitivity vector field magnetometer. The polarization of two beams of light from a laser single is compared. One of the beams has its polarization rotated by traveling through a single crystal of Yttrium-Iron-Garnet (YIG). The amount of rotation is proportional to the magnetic field strength in the YIG and the length of the YIG crystal. It should be noted that the YIG crystal is not only part of the magnetic field sensor but also plays a role in affecting the flux enhancement.

The lasar light is sent down a hole in the permalloy rods and passes through the YIG crystal. Small changes in the surrounding magnetic field result in minute changes in the polarization of the light as it passes through the YIG. These changes are detected, thus sensing changes in the magnetic field. The permalloy rods, with a composition of about 80% Ni and 20% Fe, have a higher permeability, thus focusing the magnetic field lines at the YIG. The design of the Visidyne flux concentrator is shown in Figure 1.
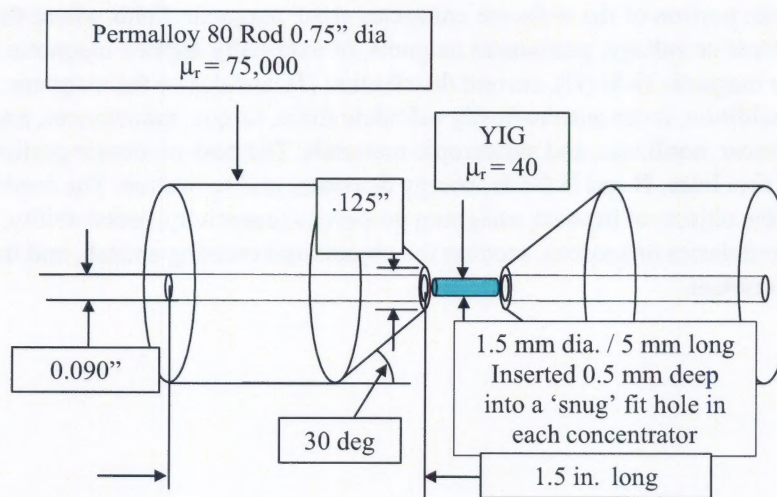

Figure 1. The Visidyne flux concentrator design.

The 0.090" diameter clearance hole down the center of the concentrator does not go all the way through to the pole end. The hole narrows to the diameter of the YIG (1.5 mm) for the last 1/2 mm, i.e. there is not a discernible air gap between the YIG and the concentrator. There are also four countersunk bolt holes in the cones of each permalloy concentrator, as shown in Figure 2. As Visidyne is not using these holes, it was requested that we not include them in our modeling.
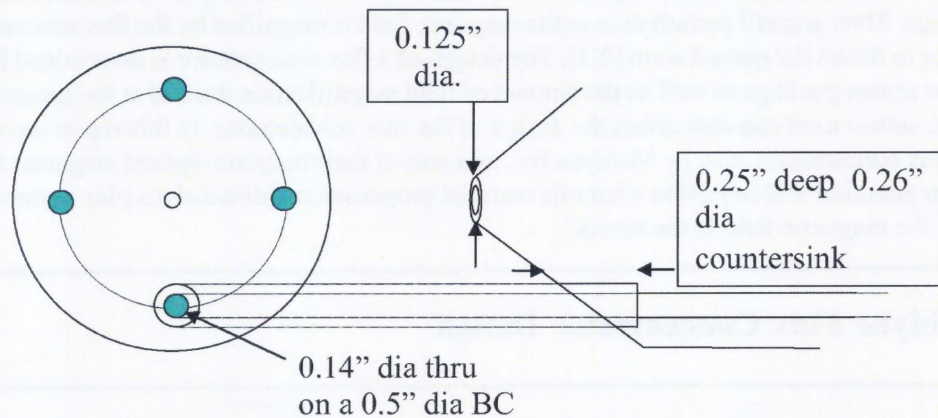

Figure 2. Bolt hole configuration in end caps of permalloy concentrators.

3. The Maxwell 3-D Magnetostatic Modeling Software

The Visidyne flux concentrator was modeled with the Maxwell 3-D software package from Ansoft Corporation. Maxwell 3-D is a finite element analysis package capable of analyzing ac magnetic, dc magnetic, and electrostatic field problems.

The 3-D DC Magnetic portion of the software computes static magnetic fields where the source origi-nates from a DC current or voltage, permanent magnets, or externally applied magnetic fields. It can directly compute the magnetic field (H), current distribution (J), and derive the magnetic flux density (B) from the H field. In addition, it can automatically calculate force, torque, inductances, and saturation in devices containing linear, nonlinear, and anisotropic materials. The post-processor portion of the software can provide plots of flux lines, B and H fields, energy densities, and saturation. The modeling process consists of drawing the objects of interest, assigning properties (coercivity, permeability, etc.) to the objects, assigning boundaries or sources, seeding the objects and creating a mesh, and then the processing of the now defined problem.

4. Results

Each model investigated involved the same fundamental sequence of steps. The first step in the analysis of the flux concentrator was to draw the model. Drawing the model consists of drawing 3-D objects and either joining them together or subtracting them from each other. This allows one to create complex objects. The permalloy rods were drawn by first making a cylinder of appropriate length. A truncated right triangle was then drawn at one end of the cylinder and swept 360 degrees around the long axis of the cylinder. The resulting solid was a truncated cone. The cone and cylinder were merged from two distinct objects into one. A cylinder was then drawn inside this object, from the base of the cylinder to the top face of the cone. Subtracting this smaller cylinder from the larger solid resulted in the shaft down the center of the rod. Finally, a mirror image of the resulting object was created. The YIG crystal is a cylinder placed slightly inside each concentrator. The objects depicted in Figure 1 are thus reproduced, to scale, in the Maxwell program (Fig. 3).
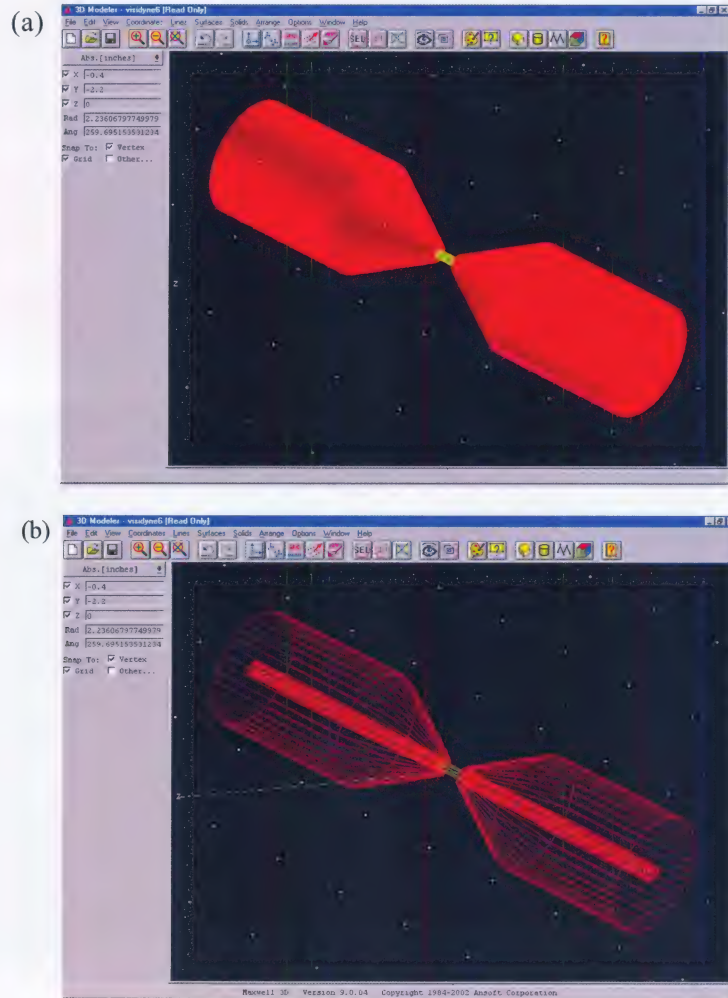
(a)

(b)

Figure 3. Three dimensional drawing of flux concentrator, (a) shaded and (b) wire frame. The red objects are permalloy, the yellow is the YIG crystal.

5

Rounded or curved objects are actually drawn with facets. A circle, for instance, would consist of line segments connected together. The greater the number of line segments, the more one approaches the smooth arc of the circle's circumference. As the number of segments or, in the case of a 3-D object, the number of facets increases, it becomes more difficult for the software to create a mesh. Meshing and calculation times will rapidly become quite long. In Figure 3b we see that a sufficient number of facets were made to approximate a relatively smooth surface on the permalloy rods and the YIG crystal. A close up of the YIG crystal is shown in Figure 4, illustrating that the YIG has a "tight fit" within the permalloy rods.
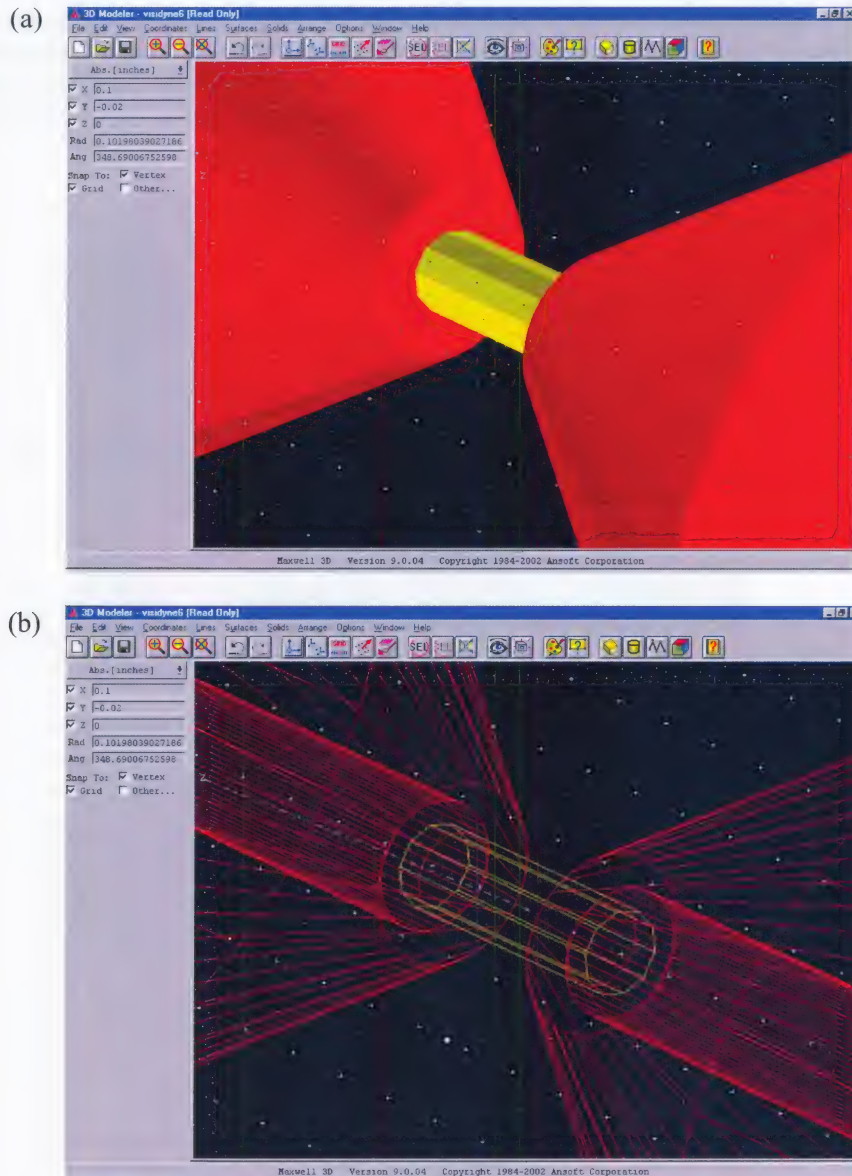
(a)

(b)

Figure 4. YIG crystal fitted inside the permalloy rods, (a) shaded and (b) wire frame.

Next, a sufficiently large region around the flux concentrator was defined as a background The material properties assigned to this background are those of a vacuum, with a relative permeability of 1. Initially we assigned a relative permeability value of 75,000 to the permalloy and 40 to the YIG. Visidyne suggested these values to us, though they expressed an uncertainty as to the exact values. We later varied these values to see what the effect would be on the enhancement of the magnetic field. We then use the 3-D boundary and source manager of the Maxwell program to assign a constant magnetic field to the background. This field was set at 100 A/m along the y-axis, the long axis of the flux concentrator. This field, then, fills all of the background.

The last step prior to performing the calculations is to seed the objects of interest and create a mesh. Care must be taken to put enough seeds in the areas of interest without actually over seeding. At the same time, one keeps calculation time down by seeding the background only enough to not distort the mesh too much across region boundaries. We seeded by volume, with no maximum element volume set. We manually seeded 30,000 elements into the background, 3000 elements into each permalloy rod, and 1000 elements into the YIG crystal. At this point the problem was fully described and ready to be solved. The program was set to solve to an error of 0.1 to 0.01%. Altogether, this study generated 630 MEG of files.

I.   Varying the Permeability of the Permalloy

The first part of the study consisted of keeping the relative permeability of the YIG crystal constant at 40 and varying the relative permeability of the permalloy from 1, the value for a vacuum, to 75,000. The permeability of the background was also kept constant at 1. We refer to this as Model 1. For each value of the permalloy permeability in Model 1, we calculated the enhancement factor and produced a map of the magnetic field lines in and around the flux concentrator. The enhancement factor is defined as the ratio of the calculate field value B_{in} at the center of the YIG crystal to the applied field. The results of the modeling that are available in the post-processor are given in SI units. We then have:

$$B = \mu_0(H + M) \text{ where } \mu_0 \times 4\pi \times 10^{-7} \text{ H/m}$$

So in a vacuum with an applied unidirectional field:

$$M = 0, \text{ and } B = \mu_0 H = (4\pi \times 10^{-7} \text{ H/m})(100 \text{ A/m}) = 12.57 \ 10^{-7} \text{ (V·s/A)(A/m)}$$

$$= 12.57 \times 10^{-7} \text{ (V·s/m}^2) = 12.57 \times 10^{-7} \text{ (Wb/m}^2) \text{ or } 12.57 \times 10^{-7} \text{ Tesla}$$

If we call this value B_{appl}, then the enhancement factor is defined as B_{in} / B_{appl}.

Plots of H always had a "bullseye" type field strength profile. A typical plot is shown in Figure 5. Plots of the **B** and **H** fields (Figs. 6–7 respectively) indicate that the fields are indeed being focused into the YIG crystal, although there are stray field lines off of edges, faces and tips as the field approaches the position of the YIG crystal. This statement holds true for all values of permalloy permeability tested in the standard model. Figures 5-7 are from the standard model, with the relative permeability of the permalloy set to 75,000. The calculated enhancement for this case was 361. Decreasing the permalloy permeability to 10,000 produced almost no change. In this case the enhancement factor was 365. This slight increase is not significant since it is within the error of our calculation. For permeability values less than 10,000, enhancement drops rapidly. The relationship between the permalloy permeability and the enhancement factor is shown in Figure 8.
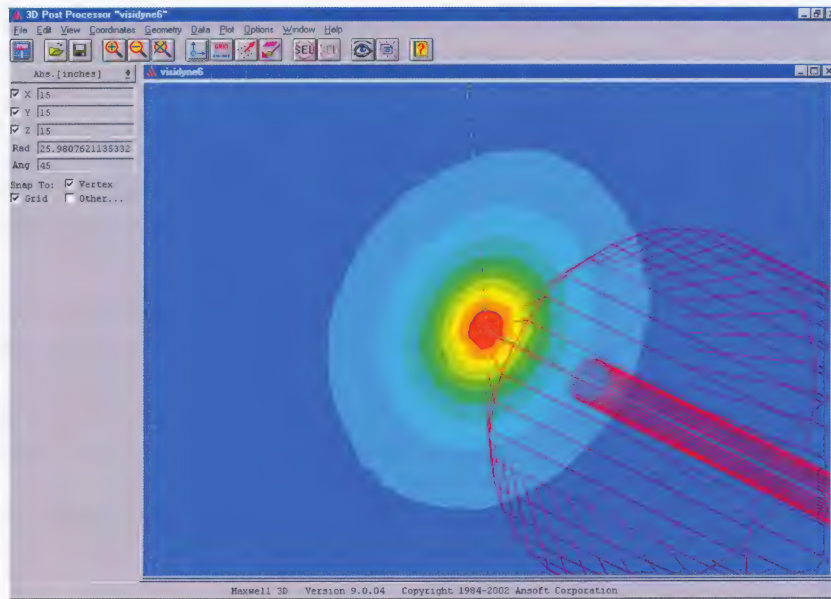
7

Figure 5. Plot of H in the x-z plane, through the origin. Progression from blue to red indicates increasing field strengths from the background to the center of the YIG.
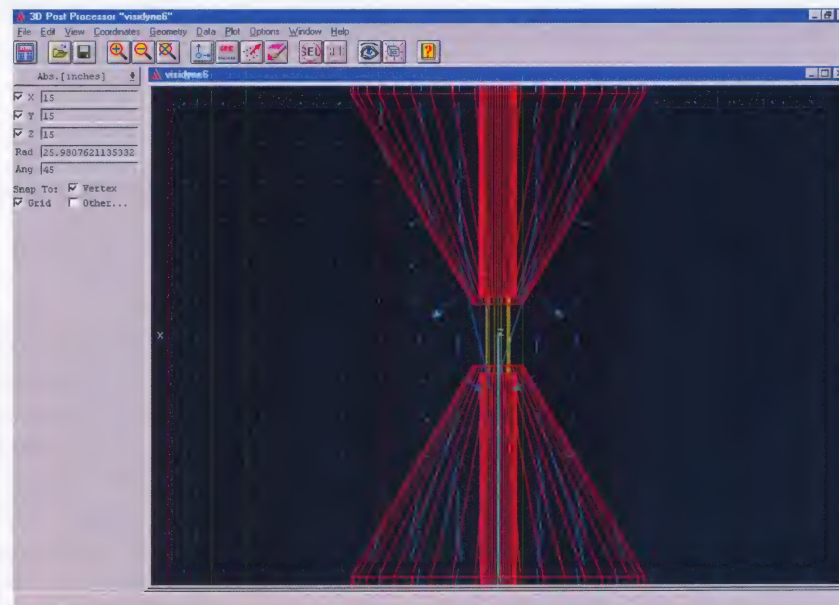

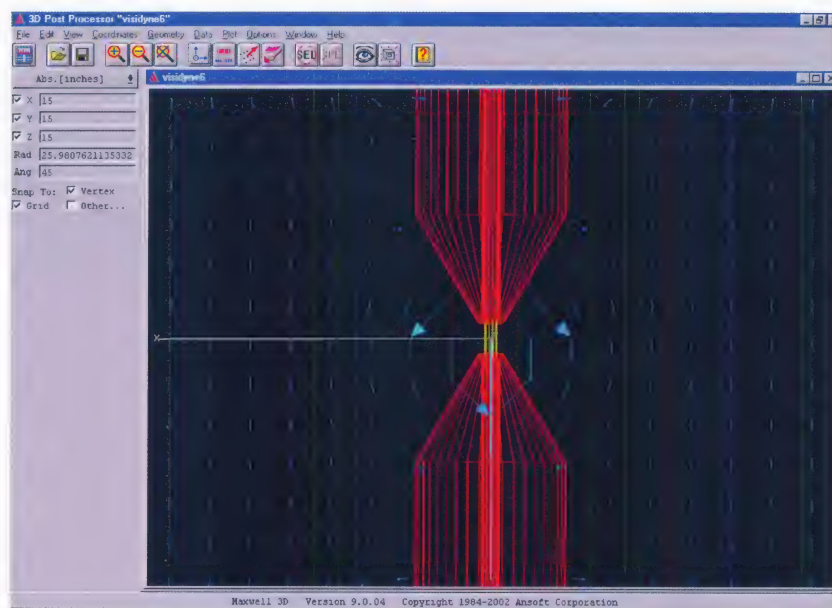Figure 6. Plot of the magnetic flux density B in the x-y plane, looking down the z-axis.

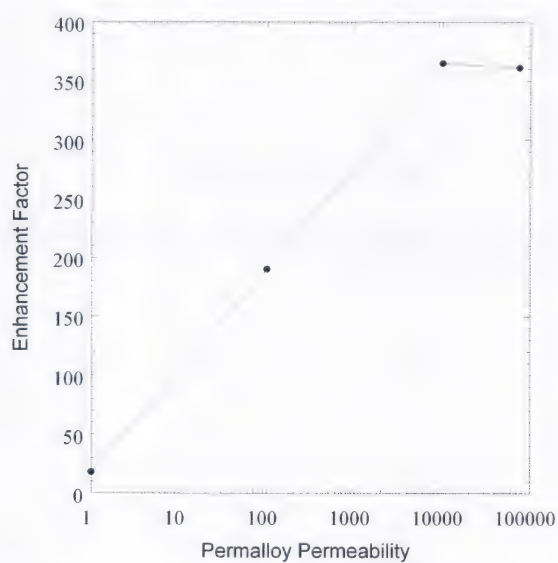Figure 7. Plot of the magnetic field strength H in the x-y plane, looking down the z-axis.

Figure 8. Plot of changes in enhancement factor as the permalloy permeability changed. Please note the x-axis is log scale. YIG permeability held constant at 40.

II.   Varying the Diameter of the Permalloy Rods

The second part of the study involved varying the diameter of the permalloy rods. The relative permeability of the YIG crystal was fixed at 40 and the diameter was varied from 0.75 in., that of Model 1, to 0.375 in. The permeability of the permalloy was fixed at 10,000. In the case where the diameter is half of the original, the seeding was altered. We manually seeded 25,000 elements into the background, 2000 elements into each permalloy rod, and 1000 elements into the YIG crystal. As shown in Figure 9, there is a gradual decrease in the enhancement factor as the diameter of the permalloy rod is decreased.
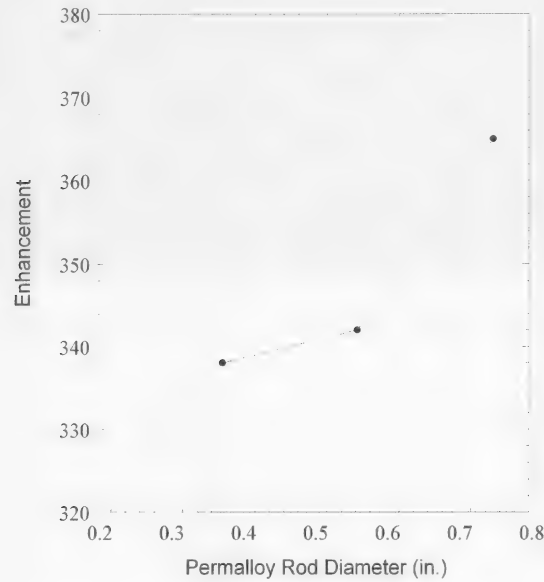

Figure 9. Plot of changes in enhancement factor as diameter of permalloy rod is changed.

III. Investigation of Optimizing the Enhancement

The last part of the study was an effort to increase the enhancement factor beyond 365. Three attempts were made. The first attempt involved preserving the overall length of the permalloy rods at 1.5 in. but changing the outer angle of the cone (Fig. 1) from 30 degrees to 20 degrees. The model was re-drawn to incorporate this change and the seeding was identical to that of the standard model. The relative permeability of the YIG crystal and the permalloy was 40 and 10,000. This resulted in an enhancement factor of 386. The second attempt maintained the 20 degree outer angle of the cone but now doubled the length of the rod. This made the total length of the permalloy pieces, rod plus truncated cone, 2.14 in. instead of the 1.5 in. of the standard model (Fig. 1). The relative permeability of the YIG and the permalloy was also the same as the first attempt, but the seeding was not increased. The mesh refining process that is part of the solution process automatically accounted for this change in dimensions. The physical model is shown in Figure 10 and can be compared to the Model 1 design in Figure 3a. The enhancement factor due to this new design was 509.

The last attempt involved returning to Model 1 and varying the relative permeability of the YIG crystal. The permeability of the permalloy was held constant at 75,000. Values of 40, 80, and 160 were used for the permeability of the YIG. We see in Figure 11 that we can greatly increase the enhancement factor, reaching a value of 1095 when the permeability of the YIG is 160.
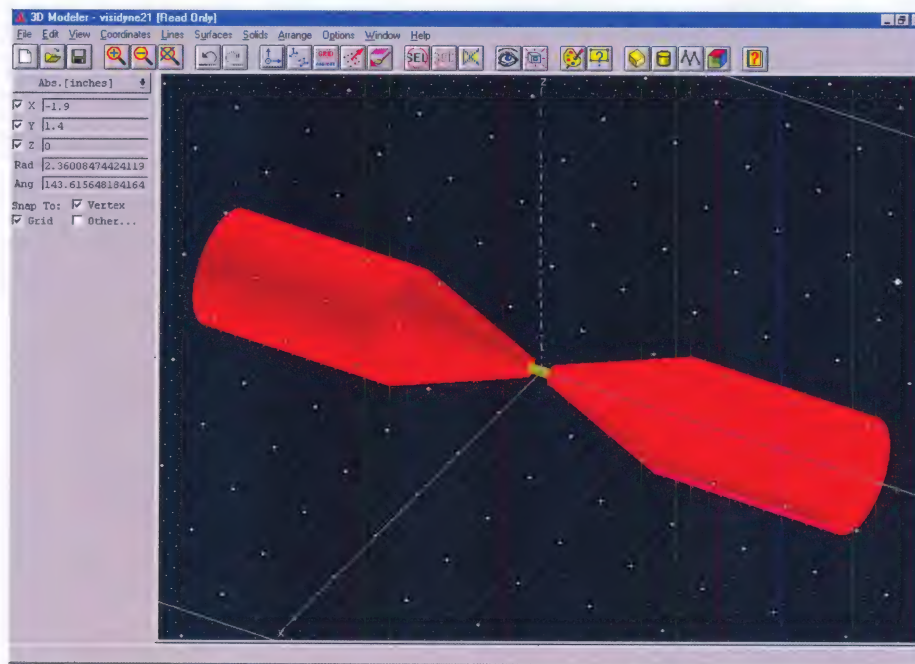

Figure 10. Physical design of flux concentrator incorporating changes of rod length and truncated cone angle.
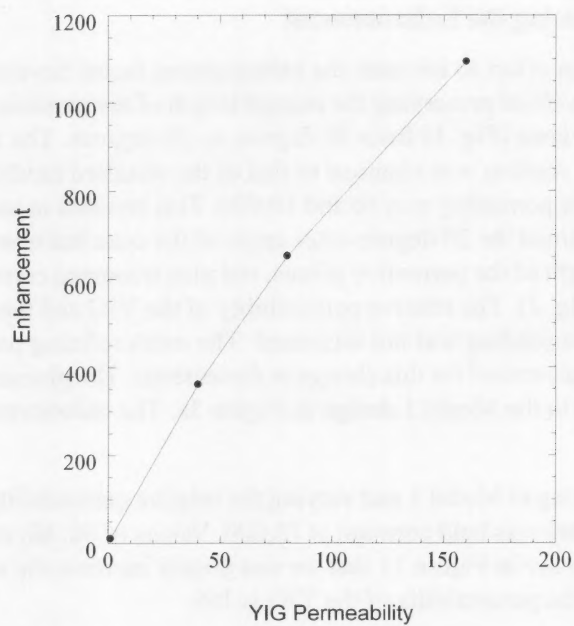
Figure 11. Plot of changes in enhancement as the relative
permeability of the YIG crystal is increased. Permeability
of the permalloy is held constant at 75,000.

5. Conclusions

Magnetic modeling of the Visidyne magnetic flux concentrator has been performed. The Maxwell 3-D finite element analysis software package from Ansoft was used. First, the Visidyne design was studied to determine the enhancement factor given the dimensions, materials, and relative permeability of their materials. We showed that with their design, an enhancement factor of 361 to 365 could be expected. We then went on to determine how variations in the dimensions and relative permeability of the flux concentrator would alter the enhancement factor. The results for varying the permeability are shown in Table 1. By setting the permeability of the permalloy to 1, we are essentially removing it from the model and arriving at the enhancement factor, 18, due only to the YIG crystal.

We did not extend our study to permalloy permeability values beyond 75,000 as we felt this would not be realistic. We showed that significantly increasing the enhancement factor at the center of the YIG could be accomplished with a change in the dimensions of the permalloy rods and truncated cones. We were able to increase the enhancement factor to 509. We also showed that an increase in the relative permeability of the single crystal YIG, if possible, could increase the enhancement factor to a greater degree than altering the dimensions of the permalloy rods and truncated cones. These results are shown in Table 2. By setting the permeability of the YIG crystal to 1, we are essentially removing it from the model and arriving at the enhancement factor, 11, due only to the permalloy when it has a permeability of 75,000. The product of the individual enhancement of the permalloy, 11, and the YIG crystal, 18, is 198. This value is considerably less than the calculated value of the combined enhancement, 363±2. Apparently multiplying the individual enhancement values only yields a rough approximation of the total enhancement value.

Table 1. Model 1 results. YIG permeability held constant at 40.

Relative Permeability of Permalloy	Enhancement Factor
1 (vacuum)	18
100	190
10,000	365
75,000	361

Table 2. Results of changing YIG permeability values. Permalloy permeability constant at 75,000.

Relative Permeability of YIG	Enhancement Factor
1 (vacuum)	11
40	361
80	653
160	1095

6. References

[1] Alan S. Edelstein and Gregory A. Fischer, *J. Appl. Phys.*, vol. 91, pp. 7795-7797, 2002.

[2] Neil Smith et al., *IEEE Trans. Magn.*, vol. 33, pp. 3385-3387, 1997.

[3] A. Jander et al., *J. Appl. Phys.*, vol. 93, pp. 8382-8384, 2003.

Distribution List

Defns Techl Info Ctr
ATTN   DTIC-OCP
8725 John J Kingman Rd Ste 0944
FT Belvoir VA 22060-6218

DARPA
ATTN G Duckworth
3701 N Fairfax Dr
Arlington VA 22203-1714

Ansoft Corp.
Four Station Square, Suite 200
Pittsburgh PA 15219-1119

Visidyne Corp.
ATTN D Rall
10 Corporate Place
Burlington MA 01803

US Army Rsrch Lab
ATTN AMSRD-ARL-CI-OK-T Techl Pub
 (2 copies)
ATTN AMSRD-ARL-CI-OK-TL Techl Lib
 (2 copies)
ATTN AMSRD-ARL-SE J Pellegrino
ATTN AMSRD-ARL-SE-S A Sindoris
ATTN AMSRD-ARL-SE-S J Eicke
ATTN AMSRD-ARL-SE-SS A Edelstein
ATTN AMSRD-ARL-SE-SS A Ladas
ATTN AMSRD-ARL-SE-SS G Fischer
 (5 copies)
ATTN AMSRD-ARL-SE-SS J Fine
ATTN AMSRL-D J Miller